

Effects of Age on Mechanical Properties of Dorsiflexor and Plantarflexor Muscles

CHRISTOPHER J. HASSON^{1,2} and GRAHAM E. CALDWELL¹

¹Biomechanics Laboratory, Department of Kinesiology, University of Massachusetts Amherst, Amherst, MA, USA; and
²Department of Biology, Northeastern University, Boston, MA, USA

(Received 4 August 2011; accepted 28 November 2011; published online 21 December 2011)

Associate Editor Thurmon E. Lockhart oversaw the review of this article.

Abstract—Redundancy in the human muscular system makes it challenging to assess age-related changes in muscle mechanical properties *in vivo*, as ethical considerations prohibit direct muscle force measurement. We overcame this by using a hybrid approach that combined magnetic resonance and ultrasound imaging, dynamometer measurements, muscle modeling, and numerical optimization to obtain subject-specific estimates of the mechanical properties of tibialis anterior, gastrocnemius, and soleus muscles from young and older adults. We hypothesized that older subjects would have lower maximal isometric forces, slower contractile and stiffer elastic characteristics, and that subject-specific muscle properties would give more accurate joint torque predictions compared to generic properties. Unknown muscle model parameters were obtained by minimizing the difference between simulated and actual subject torque-time histories under both isometric and isovelocity conditions. The resulting subject-specific models showed age- and gender-related differences, with older adults displaying reduced maximal isometric forces, slower force-velocity and altered force-length properties and stiffer elasticity. Tibialis anterior was least affected by aging. Subject-specific models gave good predictions of experimental concentric torque-time histories (10–14% error), but were less accurate for eccentric conditions. With generic muscle properties prediction errors were about twice as large. For maximum predictive power, musculoskeletal models should be tailored to individual subjects.

Keywords—Aging, Musculoskeletal modeling, Hill muscle model, Tibialis anterior, Soleus, Gastrocnemius, Triceps surae, Subject-specific, Optimization.

INTRODUCTION

The effects of nervous control signals are mediated by muscle mechanical properties such as the nonlinear force-length and force-velocity relationships of active contractile elements,^{27,32} and the nonlinear force-extension relationship of passive series elastic structures.³ Age-related changes in these properties could have a large impact on muscle function and movement coordination in older adults.³⁴ It has been shown that older muscle exhibits reduced maximal isometric force capabilities,²³ decreased contraction velocity,⁴³ and increased series elastic stiffness.⁵⁰ Dynamometer studies on single joint muscle groups show that older adults have smaller maximal isometric joint torques,⁴² exhibit shifts in the torque-angular velocity relationship towards slower velocities,⁴² and have increased joint stiffness.⁶ However, studies on how *individual* muscle mechanical properties change with aging are sparse, due to technical difficulties imposed by the redundant nature of the human muscular system^{32,62} and ethical considerations regarding direct muscle force measurement *in vivo*.

Thelen⁵⁹ simulated aging changes by altering muscle model parameters in a musculoskeletal model, illustrating that these changes go beyond muscle strength reductions alone, and include modifications of force-velocity and stiffness properties. However, this study used general age-related parameter changes, chosen from a range of studies and subject populations. Because muscle model performance is sensitive to input parameters,⁵⁴ it is important to develop subject-specific models to examine the influence of aging on muscular properties. Optimization methods can be used to estimate individual muscle properties that sum to match measured joint torque-angle and torque-angular velocity relationships.^{11,26} Such optimization

Address correspondence to Christopher J. Hasson, Department of Biology, Northeastern University, Boston, MA, USA. Electronic mail: cjhasson@neu.edu

techniques are appealing when combined with muscle-specific imaging information to constrain solutions to realistic subject-specific values. Magnetic resonance imaging can be used to measure subject-specific muscle volumes¹¹ and moment arms,⁵³ while muscle elasticity can be measured using ultrasound.²⁴

Therefore, our aim was to obtain subject-specific estimates of the mechanical properties of the major muscles controlling sagittal-plane movement at the ankle joint in young and older adults. Hill-type models were used to represent the dorsi- and plantarflexor muscles, with parameters defining the muscle force-length, force-velocity, and force-extension relationships determined by numerical optimization. Realistic constraints were imposed based on subject-specific imaging and dynamometer data sets. We hypothesized that the older subjects would have lower maximal isometric force capabilities, slower contractile properties, and stiffer elastic characteristics. It was expected that subject-specific muscle properties would give more accurate joint torque predictions compared to the use of generic properties.

METHODS

Previously, we reported left-leg dorsi- and plantarflexion torque-angle ($T\theta$), torque-angular velocity ($T\omega$), and torque-extension ($T\Delta L$) relationships from healthy, community-dwelling young (27 ± 3 years; 67 ± 7.4 kg; 1.73 ± 0.07 m; mean \pm standard deviation), and older (72 ± 5 years; 82 ± 14 kg; 1.72 ± 0.09 m) adults.³⁰ Here, we describe an optimization approach to finding subject-specific muscle model parameters that minimize the difference between musculoskeletal model and experimental joint torques over a range of isometric and dynamic conditions. Our university Institutional Review Board approved all experimental procedures.

Experimental Measurements

A Biodex dynamometer was used to measure dorsi- and plantarflexor maximal torque for construction of subject-specific $T\theta$ and $T\omega$ relations.³⁰ For $T\theta$, subjects performed maximal isometric efforts at five angles across the ankle range of motion, with the knee fixed at 100° for dorsiflexion and at two different angles for plantarflexion (90° and 180°). For $T\omega$, concentric isovelocity trials were performed at $20^\circ/s$ and from 30 to $240^\circ/s$ in $30^\circ/s$ increments, and eccentric trials were performed at -30 , -60 , and $-150^\circ/s$; the knee was fixed at 100° for dorsiflexion and 90° for plantarflexion. $T\omega$ torque data were adjusted to remove passive and inertial torque contributions and to account for $T\theta$

effects (see Hasson *et al.*³⁰ for details). Tibialis anterior (TA), gastrocnemius (GA), and soleus (SO) excitation onset times were determined from electromyograms (EMGs) recorded with preamplified ($35\times$) surface electrode pairs (Ag-AgCl; 1 cm diameter; 20 mm interelectrode distance), then amplified (input impedance: >25 M Ω at DC; CMRR: 87 dB at 60 Hz; Therapeutics Unlimited) and band-pass filtered (20–400 Hz). Torque and EMG data were sampled at 1000 Hz using a 16-bit A/D converter.

To assess muscle elasticity, subjects performed five dynamometer trials in which voluntary ankle torque was slowly increased to maximum over 30 s (see Hasson *et al.*³⁰ for details). Internal muscle kinematics were imaged by placing an ultrasound probe over the TA and the lateral GA. An automated two-dimensional spatial cross correlation algorithm⁴⁴ was used to track the motion of points on the deep aponeuroses of TA, GA, and SO to calculate dorsi- and plantarflexor series elastic element extension (ΔL_{SEE}). Torque and ΔL_{SEE} data were sampled at 30 Hz.

Musculoskeletal Model

Hill-type models consisting of contractile (CE) and series elastic (SEE) elements³² were used to represent the TA, SO, and GA muscle-tendon units (Fig. 1). The TA model lumps all dorsiflexor muscles in the anterior compartment of the leg together. CE behavior was characterized by nonlinear excitation-activation, force-length (FL), and force-velocity (FV) relationships, while the SEE had a nonlinear force-extension ($F\Delta L$) relationship (see Appendix for details). While some muscle models include parallel elasticity either as individual model parallel-elastic elements⁶⁵ or as a lumped passive elastic joint torque,⁶³ this was unnecessary here because passive contributions were removed from the experimental torque data prior to parameter determination.

Muscle-tendon lengths and moment arms were computed using SIMM models,¹⁶ scaled to each subject using measured leg lengths and sagittal-plane magnetic resonance images (1.5 Tesla; GE Sigma EchoSpeed). A phased-array coil was used with standard imaging parameters (T_1 -weighted spin echo sequence, 4 mm slice thickness with no gap, 400 ms repetition time, 11 ms echo time, 512×512 pixel resolution, 30 cm field of view). Using custom MATLAB[®] programs, the image that bisected the Achilles tendon in the sagittal plane was used to identify the ankle joint center and the TA, GA, and SO tendon lines of action⁵³ (Fig. 1). Measurements were repeated three times by the same investigator to compute the average moment arm (Table 1). The mean intra-observer standard deviation was 1.4 mm for the TA and 1.7 mm

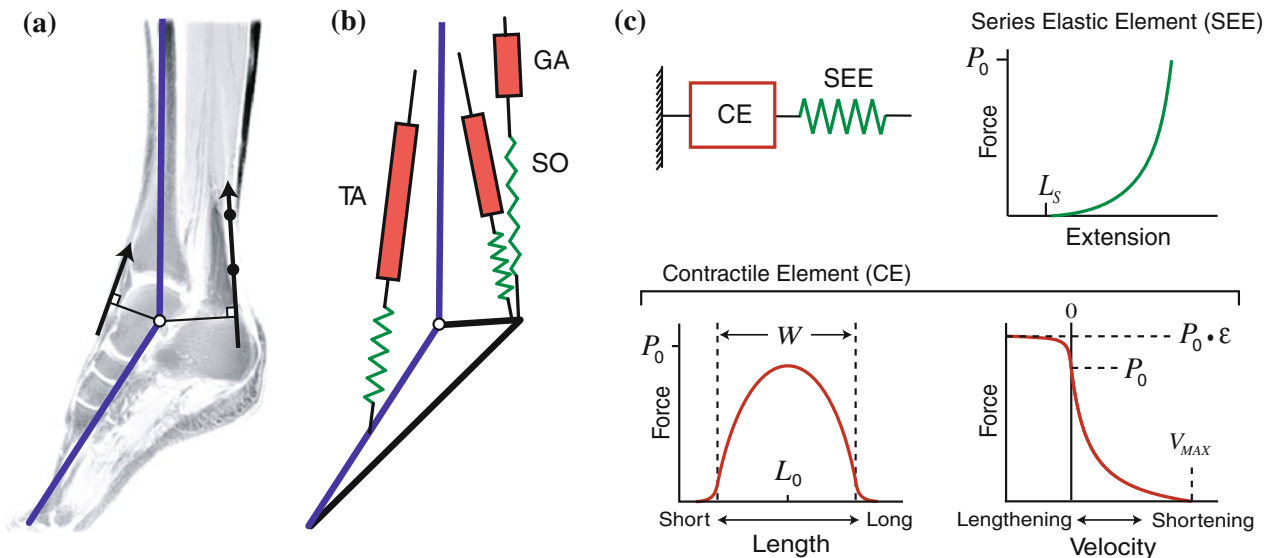


FIG. 1. (a) Example of moment arm determination for a subject using a sagittal-plane magnetic resonance image. The same moment arm was used for the GA and SO. The pixel intensities were inverted for clarity. (b) Schematic of musculoskeletal model showing muscle models for the TA, GA, and SO. (c) Muscle model and properties of the contractile element (CE) with force-length and force-velocity relations, and the series elastic element (SEE) with its force-extension relation.

TABLE 1. Measured muscle moment arms, measured contractile volumes, estimated variables used for calculation of PCSA, and anthropometric data.

Group	Mus.	MA (cm)	Volume (cm ³)	FL_{OPT}^a (cm)	θ^a (°)	PCSA (cm ²)	PCSA ratio (SO/GA)	L_{Leg} (cm)
Young male	TA	3.4 ± 0.2	256 ± 27	6.3 ± 0.3	5.0	40.7 ± 3.7	1.27	24.9 ± 3.0
	GA	4.6 ± 0.4	394 ± 75	5.0 ± 0.3	12.5	78.9 ± 12.6		
	SO	4.6 ± 0.4	423 ± 53	4.2 ± 0.2	25.0	100 ± 11.0		
Young female	TA	3.2 ± 0.3	191 ± 44	5.8 ± 0.5	5.0	33.2 ± 7.9	1.31	21.9 ± 1.1
	GA	4.4 ± 0.3	323 ± 79	4.6 ± 0.4	12.5	68.9 ± 18.9		
	SO	4.4 ± 0.3	387 ± 66	3.9 ± 0.4	25.0	90.5 ± 17.6		
Older male	TA	3.7 ± 0.2	257 ± 45	6.3 ± 0.3	5.0	40.5 ± 6.0	1.35	30.1 ± 2.0
	GA	5.0 ± 0.4	299 ± 73	5.0 ± 0.2	12.5	58.1 ± 14.7		
	SO	5.0 ± 0.4	371 ± 151	4.3 ± 0.2	25.0	79.0 ± 33.4		
Older female	TA	3.2 ± 0.2	172 ± 24	6.0 ± 0.3	5.0	28.3 ± 5.9	1.65	26.7 ± 3.4
	GA	4.5 ± 0.4	229 ± 35	4.8 ± 0.2	12.5	46.6 ± 6.5		
	SO	4.5 ± 0.4	346 ± 40	4.1 ± 0.2	25.0	77.1 ± 11.2		

Note All values are mean ± between subjects standard deviation.

Abbreviations TA: tibialis anterior (includes all anterior compartment leg muscles); SO: soleus; GA: gastrocnemius (both lateral and medial heads); L_{Leg} : leg length (knee to ankle); FL_{OPT} : optimal fiber length; θ : pennation angle; MA: muscle moment arm at the ankle.

^aEstimated from literature (see text for details).

for the GA and SO. In each sagittal-plane image, the relative ankle angle between the shank and foot segments was computed. A dorsi/plantarflexion ankle angle vs. moment arm relation was created for each muscle in the standard SIMM anatomical model. These SIMM moment arm-angle relations were scaled with the individual subject moment arm measurements so that the shape of the moment arm-angle relation was the same for all subjects, but the magnitudes of the predicted moment arms were subject-specific. For TA, the moment arm was modeled as increasing linearly with muscular force due to retinaculum stretching,

with the moment arm at MVC 35.6% longer than at rest.⁴⁷

Simulations

Isometric and isovelocity simulations were performed to predict subject-specific muscle model properties *via* numerical optimization (Fig. 2). Muscle CEs began at rest (zero force), with subsequent excitation time histories converted to muscle activation using an exponential function with a 140 ms time constant for rising activation.⁶⁵ We assumed that all subjects could

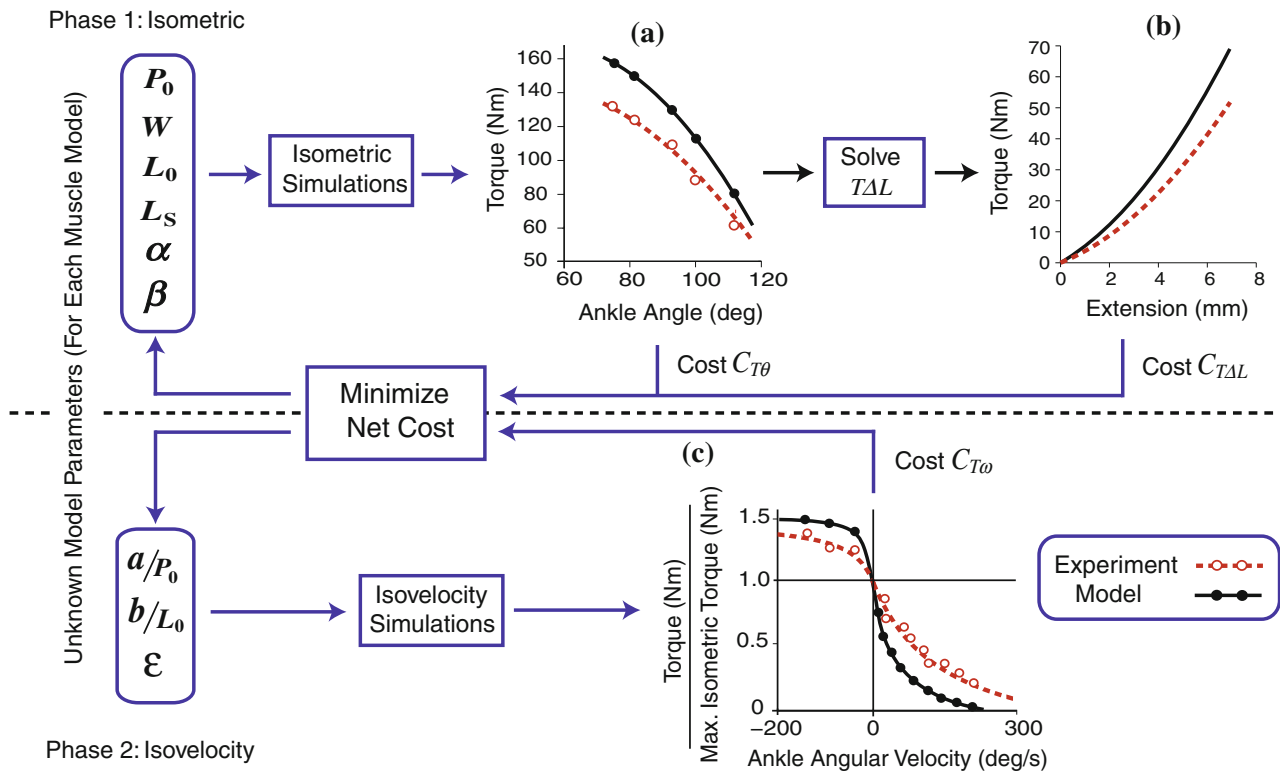


FIG. 2. Schematic of isometric (Phase 1) and isovelocitory (Phase 2) optimizations performed for each subject to obtain muscle mechanical properties. In Phase 1 the isometric muscle model parameters were found by minimizing the difference between model-generated and experimental torque data measured on a dynamometer. Experimental data included the torque vs. ankle angle relation (a) and the torque vs. series-elastic extension relation (b). The latter was measured using ultrasound. Once the isometric parameters were found, in Phase 2 the remaining velocity dependent properties were found by minimizing the difference between model and experimental torque vs. ankle angular velocity data (c). See text for more details.

maximally excite their muscles, and that the excitation was always maximal in the simulations.

For each subject, dorsi- and plantarflexion model $T\theta$ relations were constructed (Fig. 2a). A single model $T\theta$ curve entailed isometric simulations at each of the experimental ankle angles with the appropriate model knee angle. At each ankle angle, the protagonist muscles received maximal excitation for several seconds producing “isometric plateau” force, which was multiplied by the muscle moment arm to give net joint torque (plantarflexor = GA + SO torque).

Model $T\omega$ relations (Fig. 2c) were constructed similarly, with three differences: (1) the model used simulated joint angle time-histories at each experimental velocity, (2) the knee angle was set to 90° , and (3) muscle model excitation onsets were determined from experimental EMGs using a threshold of three standard deviations above baseline. Because of the temporal excitation–activation relation, muscle model activation could be sub-maximal in high-velocity trials.⁷ The peak joint torque represented a single point on the $T\omega$ curve; the set of simulations from all ankle angular velocities defined complete model dorsi- and plantarflexion $T\omega$ curves.

Model torque–extension relations were computed during the dorsi- and plantarflexion isometric simulations (Fig. 2b). An array of SEE extensions ΔL_{SEE} ranging from 0 to 80% of subject maximal extension was created. A second-order polynomial force–extension equation with α and β shape coefficients was then solved for the muscle CE forces (see Appendix). Forces were multiplied by their respective moment arms to produce model $T\Delta L$ relations in a manner similar to the model $T\theta$ and $T\omega$ relations.

Optimization of Muscle Parameters

A genetic optimization algorithm⁵⁸ was used to find the combination of muscle model parameters that minimized the differences between model and experimental $T\theta$, $T\Delta L$, and $T\omega$ data for each subject. Dual phase optimizations were performed separately for dorsi- and plantarflexion muscle groups (Fig. 2). Phase 1 searched for an optimal set of isometric CE (maximal isometric force P_0 , force–length parameters L_0 and W), and SEE (L_S , α , and β) parameters that resulted in the best match between simulated and experimental $T\theta$ and $T\Delta L$ data. Phase 2 used these optimized isometric

parameters while finding the CE force–velocity parameters (a/P_0 , b/L_0 , and ε) that gave the best simulation match to the $T\omega$ data. In the genetic algorithm, the number of population members per generation was equal to 10 times the number of unknown parameters. The algorithm finished when all population member costs differed by less than 0.001 Nm.

Optimization Constraints

To avoid unrealistic solutions for muscle parameters, several constraints were used in the optimization process. Computed SO and GA physiological cross-sectional areas (PCSAs) were used to constrain the possible choices for optimized SO and GA P_0 values, with

$$PCSA = \frac{Vol}{FL_{OPT}} \cos \theta \quad (1)$$

where Vol is the volume of the contractile tissue, θ is the pennation angle, and FL_{OPT} is the optimal muscle fiber length. For each subject, Vol was measured for TA, GA, and SO using magnetic resonance imaging (Table 1; see Hasson *et al.*²⁹ for details). Values for θ were based on Wickiewicz *et al.*,⁶¹ although θ can vary with location within the triceps surae muscles,¹ and with muscular force magnitude.⁴⁶ Although these literature-based resting θ values may introduce small errors ($\sim 5\%$) in PCSA computations, this is not critical given their use as a constraint only. FL_{OPT} was computed by multiplying muscle–tendon length by FL_{OPT} /muscle–tendon length ratios, calculated for TA from Spoor *et al.*⁵⁷ and for SO and GA from Out *et al.*⁵² When optimizing P_0 , the SO P_0 /GA P_0 ratio could only vary by $\pm 15\%$ of the computed $PCSA_{SO}/PCSA_{GA}$ ratio.

Optimal CE length L_0 was constrained to be within $\pm 25\%$ of the literature-based FL_{OPT} . The parameter W could vary to produce force–length widths between 0.8–1.2 L_0 (highly pinnate muscles) and 0.2–1.8 L_0 (parallel-fibred),⁶⁴ with SO W limited to be within $\pm 20\%$ of the GA W . The model SO force–extension coefficients were constrained to be within $\pm 15\%$ of GA.⁸ The force–velocity coefficient a/P_0 could vary between 0.15 (slow) and 0.6 (fast), while b/L_0 could vary between 1.0 (slow) and 8 s⁻¹ (fast).¹⁴ The eccentric plateau ε could range from 1.1 to 3 (slightly more than Epstein and Herzog²¹ and Cook and McDonagh¹⁵), with GA and SO ε limited to be within $\pm 25\%$ of each other. Maximum CE shortening velocity v_{Max} could vary between 9 and 15 L_0/s .⁵⁴

Optimization Phase 1

For each subject, a best root-mean-squared (RMS) fit between model and experimental $T\theta$ and $T\Delta L$ data sets was obtained by minimizing costs $C_{T\theta}$ and $C_{T\Delta L}$,

respectively. Thus, the net cost was $f(\vec{X}) = C_{T\theta} + C_{T\Delta L}$, where \vec{X} is the vector of isometric model parameters (one vector per muscle), with $\vec{X} = [P_0, L_0, W, L_S, \alpha, \beta]$. At each optimization step, a complete set of isometric torque simulations was performed with a candidate vector of muscle parameters, with second-order polynomials fit to the model and experimental $T\theta$ and $T\Delta L$ data. These curves were evaluated at 1° ankle angle increments over each subject's range of motion ($T\theta$), and at 1% increments from zero to 80% L_S ($T\Delta L$). The $T\theta$ cost $C_{T\theta}$ was

$$C_{T\theta} = \sqrt{\sum_{i=1}^N (T_{\theta_i}^{MOD} - T_{\theta_i}^{EXP})^2} \quad (2)$$

and the $T\Delta L$ cost $C_{T\Delta L}$ was

$$C_{T\Delta L} = \sqrt{\sum_{i=1}^N (T_{\Delta L_i}^{MOD} - T_{\Delta L_i}^{EXP})^2} \quad (3)$$

where T_{θ_i} is the maximal isometric torque at joint angle i , $T_{\Delta L_i}$ is the torque produced at SEE extension i , and N is the number of evaluated data points (MOD: model; EXP: experimental).

Optimization Phase 2

In the second phase, best fitness was obtained by minimizing a single cost $C_{T\omega}$ associated with the RMS difference between model and experimental $T\omega$ equations. The net cost was $f(\vec{X}) = C_{T\omega}$, where $\vec{X} = [a/P_0, b/L_0, \varepsilon]$. Each $T\omega$ equation was in the form of a rectangular hyperbola over the interval $[-200^\circ/s$ (eccentric), 300°/s (concentric)]. The $T\omega$ cost $C_{T\omega}$ was

$$C_{T\omega} = \sqrt{\sum_{i=1}^N (T_{\omega_i}^{MOD} - T_{\omega_i}^{EXP})^2} \quad (4)$$

where T_{ω_i} is the maximal torque produced for joint angular velocity i , and N is the number of evaluated data points at 1°/s intervals ($N = 500$).

Model Predictions

Additional simulations were performed for each subject to determine how well the optimized muscle properties predicted experimental torque time-histories. The parameter identification process used only the peak isometric and isovelocity torques, a small subset of the experimental data. For model evaluation, joint-torque time histories were simulated for each isovelocity trial using the optimized subject-specific muscle properties. For each simulation the RMS error between the model and experimental torques was

computed from the initial excitation to the end of the constant-velocity period of joint motion, expressed relative to maximum isometric torque.

To assess the model's sensitivity to the use of subject-specific muscle model parameters, torque predictions were also made with generic muscle parameters drawn from two sources: (1) the default properties used in SIMM¹⁶ and (2) age-specific averaged values for the subjects in the present study (MEAN). In the SIMM software, the shapes of the FL , FV , and $F\Delta L$ relations were the same for all muscles, but differed slightly from our model formulation. Therefore, our equations were fit to the SIMM relations using a least squares approach, and the resulting generic parameters for L_0 , L_S and the FL , $F\Delta L$, and FV relations were used in model simulations for each subject. For both generic sets of properties, subject-specific values for P_0 were retained, thereby focusing the analysis on other aspects of the FL , FV , and $F\Delta L$ relations.

Data Analysis and Statistics

Linear mixed-effects models were used to assess age and gender differences for the optimized FL , $F\Delta L$, and FV properties for each muscle, with subject as a random factor. For $F\Delta L$ the linear stiffness at a force level of 400 N (K_{400}) was compared (other force levels gave similar results). A separate analysis compared the prediction errors between each subject's model and experimental isovelocity time-series data, with age and parameter-type (subject-specific, SIMM, and MEAN) as factors (here data were collapsed across genders). Mixed-model-based t -tests ($p < 0.05$) were used for pairwise comparisons. One young male subject was excluded from the plantarflexion optimizations due to technical issues affecting the torque measurements.

RESULTS

Muscle Properties

The dual-phase optimization process was successful in computing subject-specific FL , $F\Delta L$, and FV relations (Fig. 3). The mean $T\theta$ costs (Eq. 2) were 0.24 ± 0.27 Nm (dorsiflexion), 3.9 ± 5.4 Nm (plantarflexion; knee = 90°), and 3.4 ± 3.0 Nm (plantarflexion; knee = 180°). The mean $T\Delta L$ costs (Eq. 3) were 0.12 ± 0.08 Nm (dorsiflexion) and 0.5 ± 0.5 Nm (plantarflexion). The mean $T\omega$ costs (Eq. 4), normalized to maximal isometric torque, were 0.13 ± 0.04 (dorsiflexion) and 0.15 ± 0.06 (plantarflexion).

Isometric FL Parameters

There were no age- or gender-related differences in P_0 for TA, but for GA and SO there were interactions

between age and gender (Table 2). For both plantarflexor muscles, older males were weaker than younger males (GA: $p = 0.001$; SO: $p = 0.004$), but young and older females were not different (GA: $p = 0.710$; SO: $p = 0.463$). Older adults had a narrower TA force-length relation (smaller W), but a wider GA relation. For SO, older adults had a longer L_0 .

$F\Delta L$ Parameters

For TA and GA, males had longer L_S values than females. For SO K_{400} , there was an age by gender interaction showing stiffer SO values in older males ($p = 0.003$), but no age differences for females ($p = 0.670$). For GA K_{400} there was a main effect of age, with greater stiffness in older adults. Older adults displayed greater non-linearity in the $F\Delta L$ relations for both GA and SO, indicated by the greater shape coefficient α ($p = 0.033$ SO; $p = 0.034$ GA).

Dynamic FV Parameters

For TA older adults had slower contractile properties than younger adults (Table 3), as reflected by smaller b/L_0 , ε , and v_{Max} . For GA, there were age by gender interactions, such that older males had smaller a/P_0 and b/L_0 values compared to young males (a/P_0 $p = 0.016$; b/L_0 $p < 0.001$), but no age differences for females (a/P_0 $p = 0.684$; b/L_0 $p = 0.916$).

Model Predictions

Simulated isovelocity torque-time histories using subject-specific muscle properties gave small to moderate prediction errors (Fig. 4). The optimized subject-specific models gave mean errors between 10 and 14% across age and muscle groups in concentric isovelocity trials, with eccentric predictions less accurate (17–29% error; Fig. 5). For generic muscle properties SIMM and MEAN (Tables 2 and 3), both concentric and eccentric errors were significantly higher than with subject-specific parameters ($p < 0.001$). There were no age-related differences in error across all models ($p > 0.431$). Errors were larger for plantarflexion compared to dorsiflexion for concentric and eccentric conditions (muscle group main effect; $p < 0.05$). For concentric trials there was an interaction, with errors larger using generic muscle properties in all cases ($p < 0.001$) except for dorsiflexion, in which there was no difference between subject-specific and MEAN errors ($p = 0.348$).

DISCUSSION

A methodology was developed that combined muscle imaging, dynamometer measurements, muscle

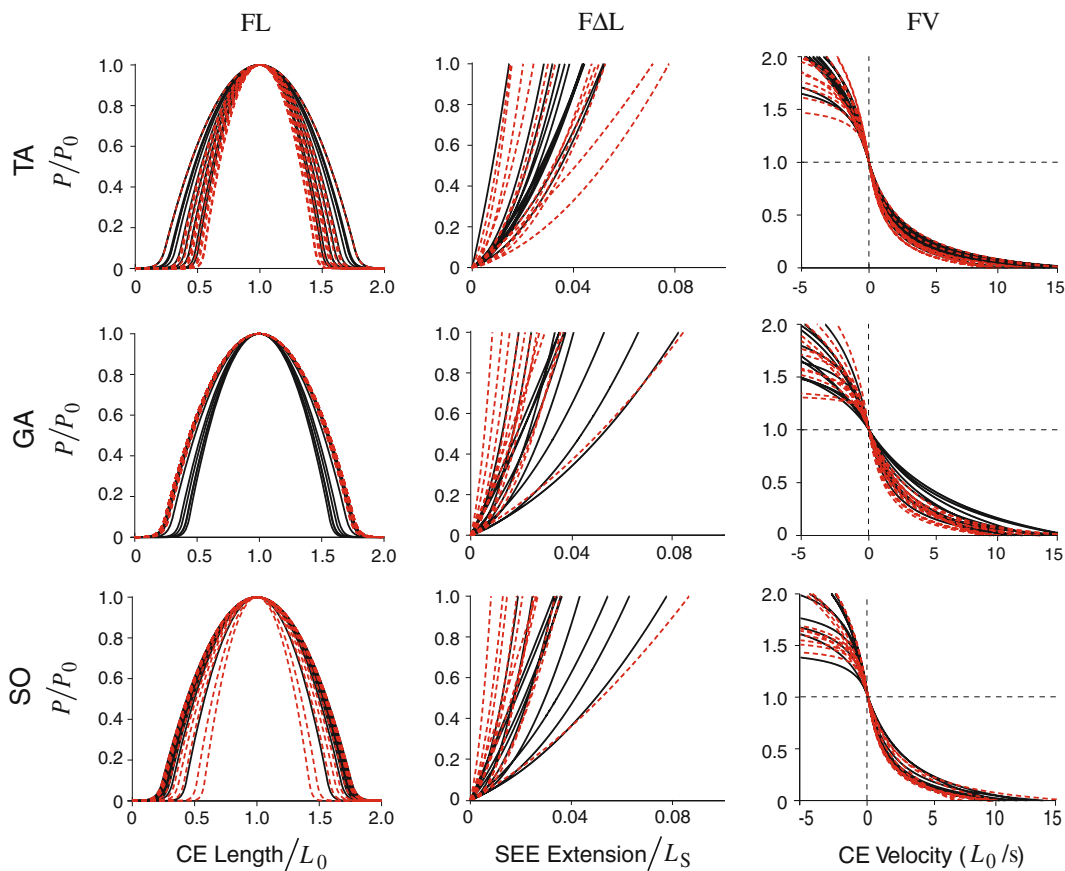


FIG. 3. Optimized force–length (*FL*; left column), force–extension (*F Δ L*; middle column), and force–velocity (*FV*; right column) relations for the TA (top row), GA (middle row), and SO (bottom row) muscle models for each young (solid black lines) and older (dashed red lines) adult.

modeling, and numerical optimization to obtain subject-specific estimates of human muscle mechanical properties. We used this methodology to examine age-related differences in the properties of the dorsiflexor and individual plantarflexor muscles, and tested how well subject-specific muscle properties could predict experimental joint torque–time histories compared with the use of generic properties.

As hypothesized, older adults displayed differences in a variety of muscle properties compared to young adults; however, some differences were gender-specific. Specifically, it was expected that the older subjects would have lower maximal isometric force capabilities, slower contractile properties, and stiffer elastic characteristics. The results showed that older males had significant decreases in maximal isometric force capability P_0 for both GA and SO compared to the younger males. Older adults had altered force–length properties, stiffer elastic elements in GA and SO (males only), and slower velocity-dependent properties for TA and GA (males only). It was also hypothesized that models with subject-specific muscle properties would give more accurate joint torque predictions than with

generic properties. The optimized subject-specific models gave relatively good predictions of dorsi- and plantarflexion experimental isovelocity torque–time histories for concentric efforts, but were less accurate for eccentric conditions. Prediction errors were about twice as large when using generic muscle properties.

Muscle Mechanical Properties

Isometric *FL* Parameters

The modeling results showed age-related decrements in P_0 for the GA and SO in males but not females. Similar age and gender interactions have been reported for maximal isometric plantarflexor torque,⁴⁰ and could be explained by age-related decreases in male testosterone concentrations,²⁸ which leads to decreased muscle mass.⁵ There were no age or gender differences for TA P_0 , which agrees with previous research showing no age-related declines in maximal dorsiflexion torque⁵⁶ (but disagrees with others⁴²). These disparate findings are most likely due to subject populations; our relatively active older adults may

TABLE 2. Optimized muscle mechanical properties for Phase 1 (isometric simulations).

Muscle	Group	P_0 (N)	Force-length (FL)		Force-extension ($F\Delta L$)			K_{400} (N/ Δ cm)
			L_0 (cm)	W	L_S (cm)	α	β	
TA	YM	666 ± 244	7.0 ± 1.2	0.72 ± 0.08	24.1 ± 1.1	605 ± 256	15 ± 20	1067 ± 217
	YF	562 ± 157	6.5 ± 1.0	0.62 ± 0.09	21.7 ± 2.3	449 ± 306	7 ± 3	894 ± 206
	OM	534 ± 105	6.7 ± 1.4	0.57 ± 0.12	23.9 ± 1.6	817 ± 947	11 ± 10	928 ± 489
	OF	588 ± 240	6.5 ± 0.6	0.58 ± 0.08	22.5 ± 1.6	1255 ± 1277	6 ± 3	1257 ± 492
	Age effect	0.516	0.770	0.020*	0.637	0.144	0.551	0.254
	Gender effect	0.762	0.453	0.238	0.014*	0.678	0.177	0.742
	Interaction	0.332	0.805	0.178	0.468	0.385	0.764	0.295
GA	YM	1637 ± 714	5.8 ± 0.8	0.70 ± 0.09	37.0 ± 2.5	311 ± 293	10 ± 8	809 ± 242
	YF	786 ± 272	5.6 ± 0.6	0.71 ± 0.08	33.6 ± 2.7	764 ± 797	13 ± 9	891 ± 270
	OM	615 ± 267	6.3 ± 0.2	0.79 ± 0.01	36.7 ± 1.6	2936 ± 2542	15 ± 18	1288 ± 387
	OF	697 ± 280	5.9 ± 0.3	0.79 ± 0.02	34.9 ± 2.0	1174 ± 1561	16 ± 13	993 ± 874
	Age effect	0.004*	0.094	0.005*	0.556	0.034*	0.490	0.015*
	Gender effect	0.036*	0.233	0.760	0.012*	0.337	0.695	0.341
	Interaction	0.013*	0.747	0.812	0.411	0.112	0.836	0.051
SO	YM	1832 ± 785	4.5 ± 0.9	0.74 ± 0.03	24.4 ± 1.9	310 ± 280	11 ± 9	1340 ± 331
	YF	953 ± 351	4.4 ± 0.4	0.75 ± 0.08	22.1 ± 2.6	756 ± 821	13 ± 10	1518 ± 514
	OM	828 ± 344	5.2 ± 0.4	0.65 ± 0.14	24.4 ± 1.4	3184 ± 2866	15 ± 19	2368 ± 819
	OF	1172 ± 489	4.8 ± 0.6	0.75 ± 0.08	23.3 ± 1.5	1140 ± 1420	16 ± 14	1942 ± 1294
	Age effect	0.079	0.043*	0.244	0.459	0.033*	0.511	0.013*
	Gender effect	0.222	0.292	0.218	0.051	0.275	0.760	0.278
	Interaction	0.009*	0.681	0.232	0.467	0.096	0.977	0.044*
TA	SIMM	674	6.8	0.54	24.1	0	37.4	1049
GA	SIMM	1914	4.4	0.54	28.2	0	37.4	1049
SO	SIMM	3586	5.4	0.54	39.1	0	37.4	1049

Abbreviations TA: tibialis anterior (includes all anterior compartment leg muscles); GA: gastrocnemius; SO: soleus; YM: young male; YF: young female; OM: older male; OF: older female; P_0 : maximum isometric force capability; L_0 : optimal contractile element length; W : width of force-length relation; L_S : series-elastic element slack length; α , β : coefficients defining series-elastic element force-extension relation; K_{400} : slope of force-extension relation at 400 N; SIMM: parameters taken from a freely available model of the lower limb² used in the musculoskeletal modeling software SIMM.¹⁶

*Significant at $p < 0.05$.

have better preserved dorsiflexor strength through daily activities like walking.

Previous work has examined age-related changes in the torque-angle ($T\theta$) relation,⁴² but to our knowledge, age-related changes in individual muscle force-length (FL) relations have not been examined in humans. For older adults the model predicted a narrower FL relation (smaller W) for the TA but a wider relation for the GA, compared to young. This could stem from age-related differences in muscle moment arm vs. joint angle relations,⁴² which could be driven by changes in tendon-routing and/or alterations in connective tissue properties.³⁹ Such changes would not be captured by the present model, since the shape of the moment arm vs. joint angle relation was the same for all subjects. Older adults were predicted to have longer optimum SO fiber length (L_0) compared to young, which runs counter to expectations from studies showing an age-related decrease in the number of in-series sarcomeres.⁴⁹ This discrepancy may again be due to age-related changes in moment arms, which would have

altered the $T\theta$ relations that the model was attempting to fit.

FAL Parameters

For the force-extension ($F\Delta L$) relation, the model predicted the GA and SO to be stiffer in older adults, with no age-related differences for TA. Such an increase in plantarflexor stiffness is supported by the literature.⁵¹ The lack of age-related differences in TA stiffness could reflect relatively well-preserved TA function, as TA strength (P_0) was maintained in the older adults. Although the GA was stiffer in both genders, the SO was stiffer in older males only. Such SO versus GA differences might be related to size and fiber composition, as slow-twitch muscle fibers are stiffer than fast-twitch.⁶⁰ Note that the modeled series elastic component stiffness represents the lumped elasticity within the external tendon, internal aponeurosis, and sarcomeres. The model also showed that males had longer TA and GA series-elastic slack lengths

TABLE 3. Optimized muscle mechanical properties for Phase 2 (isovelocity simulations).

Muscle	Group	a/P_0	b/L_0 (s ⁻¹)	ε	v_{Max} (L ₀ /s)
TA	YM	0.18 ± 0.06 ^L	2.17 ± 0.37	2.58 ± 0.53 ^U	12.8 ± 2.6
	YF	0.18 ± 0.04 ^L	2.30 ± 0.39	2.93 ± 0.14 ^U	13.2 ± 2.5
	OM	0.16 ± 0.02 ^L	1.66 ± 0.35	2.18 ± 0.50	10.5 ± 2.3
	OF	0.16 ± 0.02 ^L	1.84 ± 0.53	2.49 ± 0.56	11.2 ± 2.1
	Age effect	0.287	0.010*	0.039*	0.042*
	Gender effect	0.866	0.365	0.095	0.568
	Interaction	0.978	0.885	0.918	0.854
GA	YM	0.49 ± 0.11	6.31 ± 1.71	2.45 ± 0.53	12.7 ± 2.1
	YF	0.23 ± 0.09	2.73 ± 0.86	2.39 ± 0.57	12.2 ± 2.2
	OM	0.27 ± 0.16	2.77 ± 1.43	2.06 ± 0.74	10.9 ± 2.4
	OF	0.27 ± 0.17	2.65 ± 1.28	2.39 ± 0.65	10.6 ± 2.6
	Age effect	0.120	0.004*	0.464	0.107
	Gender effect	0.038*	0.004*	0.623	0.672
	Interaction	0.041*	0.006*	0.477	0.889
SO	YM	0.20 ± 0.11 ^L	2.06 ± 0.99	2.42 ± 0.51	10.6 ± 1.5
	YF	0.17 ± 0.05 ^L	1.74 ± 0.74	2.43 ± 0.64	9.8 ± 1.1
	OM	0.25 ± 0.16 ^L	2.01 ± 1.00	2.11 ± 0.71	8.6 ± 1.2
	OF	0.18 ± 0.07 ^L	1.71 ± 0.50	2.32 ± 0.62	9.7 ± 2.7
	Age effect	0.524	0.908	0.437	0.189
	Gender effect	0.330	0.381	0.666	0.831
	Interaction	0.675	0.974	0.702	0.225
TA	SIMM	0.25	2.53	1.80	10.0
GA	SIMM	0.25	2.53	1.80	10.0
SO	SIMM	0.25	2.53	1.80	10.0

Note Superscripts L and U indicate that for some subjects the optimized parameter values were against either a lower or upper constraint boundary, respectively.

Abbreviations TA: tibialis anterior (includes all anterior compartment leg muscles); GA: gastrocnemius; SO: soleus; YM: young male; YF: young female; OM: older male; OF: older female; a/P_0 and b/L_0 : shape coefficients for force–velocity relation; ε : eccentric plateau of force–velocity relation; v_{Max} : maximum contraction velocity; SIMM: parameters taken from a freely available model of the lower limb² used in the musculoskeletal modeling software SIMM.¹⁶

*Significant at $p < 0.05$.

(L_S) compared to females, possibly due to gender differences in limb length (Table 1).

Dynamic FV Parameters

There was an age-related decrease in TA velocity-dependent force capability for both concentric and eccentric velocities. Specifically, the model predicted a decrease in the maximal shortening velocity v_{Max} and the related b/L_0 shape parameter, consistent with the well-known age-related decrease in the size and/or number of fast-twitch Type II muscle fibers.³⁷ For the GA there was an age by gender interaction, with older males having smaller a/P_0 and b/L_0 compared to young males, but no age differences among females. A smaller shape parameter a/P_0 makes the FV relation more concave, decreasing the relative force for a given shortening velocity. Again this gender interaction could be the result of an older female group which overall showed less age-related changes than the males.

For some subjects, values for TA and SO a/P_0 were close to or against the lower constraint boundary

($a/P_0 = 0.15$). According to Diffie *et al.*,¹⁷ slower muscles typically have higher degrees of curvature in the force–velocity relation, with correspondingly smaller a/P_0 values that could approach 0.10. Compared to the GA, the TA and SO have larger percentages of slow-twitch fibers (~70%³¹ and ~88%,³⁸ respectively), which agrees with the trend in the model a/P_0 estimates. However, our lower constraint boundary may have been conservative for some subjects. Also, the young subject TA eccentric plateau ε was in some cases against the upper constraint boundary ($\varepsilon = 3$), which is above literature reports.¹⁵ This could be due to (1) ε defining a true force plateau, compared to studies in which the eccentric force rises past ε at a constant slope,⁵⁴ (2) the use of fewer eccentric data points in the model fits compared to concentric (3 vs. 10 points), and (3) eccentric trials not reaching the same high velocities as concentric.

Prediction Errors

Simulations were performed to determine how well a model with optimized subject-specific muscle properties

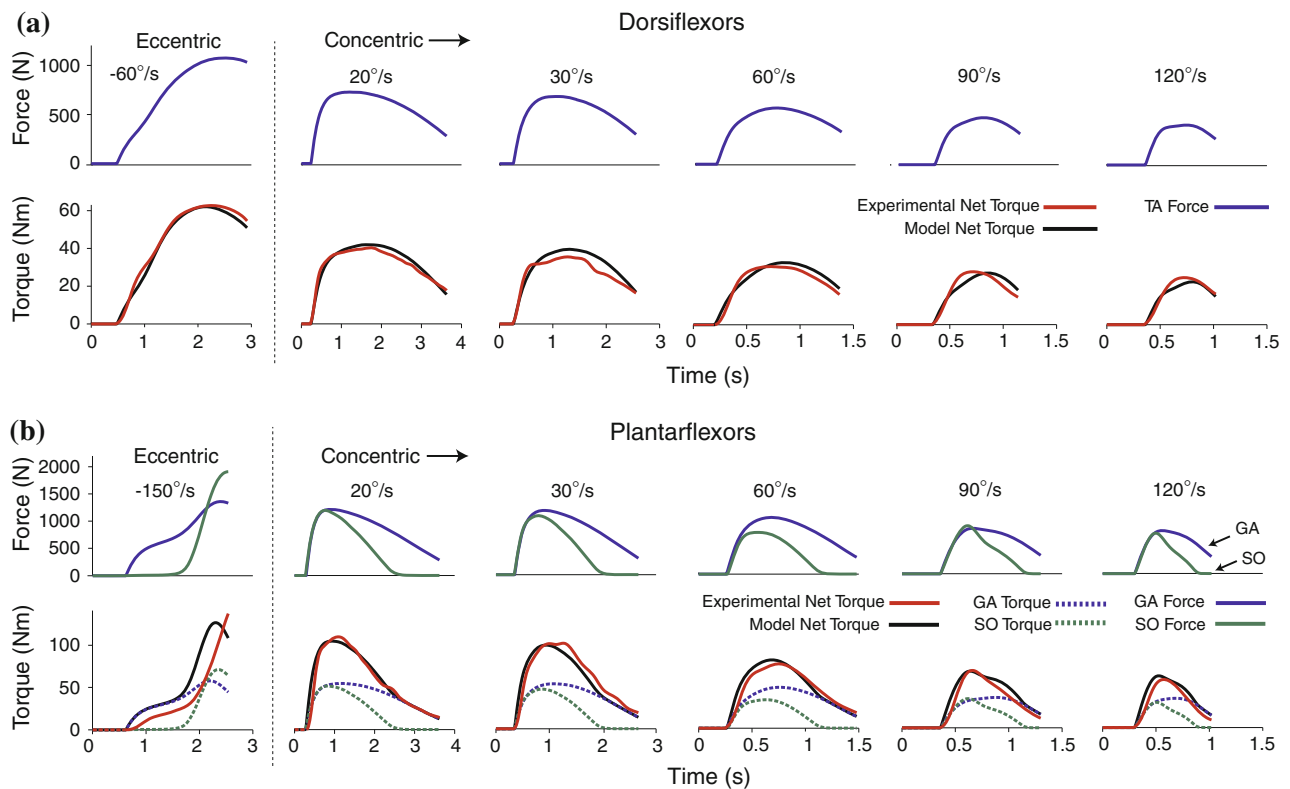


FIG. 4. Comparison between optimized musculoskeletal model and experimental net joint torques for a subset of dorsiflexor (a) and plantarflexor (b) isovelocity trials for one subject. This subject had a relatively small RMS error between the model predictions and experimental data.

could predict experimental torque time-histories. Prediction errors were relatively small for concentric conditions (10–14%), but greater for eccentric conditions (17–29%). Part of this increase is an artifact because errors are expressed relative to maximal isometric torque, with eccentric torques on average 1.37 times above the maximal isometric torque and concentric torque always below due to force–velocity effects.³⁰ This artifact would explain eccentric errors increasing to about 14–21%. The additional error could be due to sub-maximal eccentric activation,²⁰ present in the experimental trials but not the simulated ones. In general, eccentric contractions are more variable than concentric, possibly due to non-uniform sarcomere behavior,⁴⁸ which would lead to increased predictions errors due to muscle dynamics not included in the model.

Other studies have used optimization techniques to “calibrate” musculoskeletal model parameters to individual young adults²⁴ including the “EMG driven” models of Buchanan and colleagues.^{10,55} Buchanan reported prediction errors of ~9% and ~10–15% for ankle torque during locomotion in healthy young adults and older stroke patients, respectively. Our 10–14% concentric prediction errors are similar to these earlier studies. Our larger eccentric errors may be due to differences in experimental conditions. *In vivo* ultrasound

measurements during human locomotion show near-isometric behavior of plantarflexor fascicles,²⁵ while our dynamometer trials exhibited sustained eccentric muscular efforts with high lengthening velocities and torques.¹² Also, we normalized torque prediction errors to each subject’s maximal isometric torque, while Buchanan normalized errors to the peak-to-peak joint torque range during each experimental trial. If we normalize our data this way concentric errors “increase” to 17–18% (young–old; dorsiflexion) and 24–27% (young–old; plantarflexion). These “larger” errors are in part due to high velocity trials with lower peak torques, in which even a small absolute RMS error results in relatively large normalized error. Indeed, if the highest three concentric velocities are excluded, errors “decrease” to 15–17% (dorsiflexion) and 18–20% (plantarflexion). Thus error comparisons using this individual trial normalization are muddled by contractile velocity differences between locomotion and dynamometer trials.

Model accuracy was not affected by age, but torque-time predictions became worse when generic (SIMM or MEAN) muscle properties were used instead of subject-specific. This expected but important finding should be considered when modeling the musculoskeletal system. The increased error with generic properties was partly due to a shift in the force–length operating range

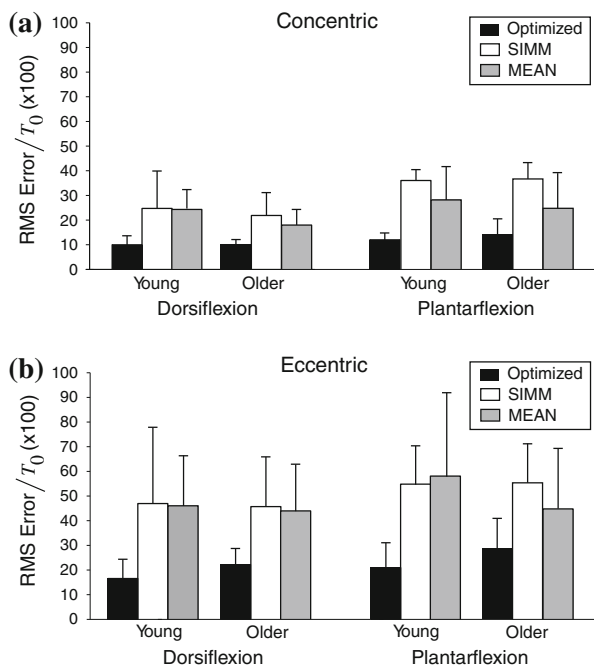


FIG. 5. Average RMS error between model and experimental torque time histories across subjects for concentric (a) and eccentric (b) kinematic conditions. The RMS error is expressed as a percentage of each subject's maximum isometric torque (T_0). Error bars represent between-subjects standard deviations. Shown are the results when using optimized (subject-specific) muscle properties and generic values obtained from either the musculoskeletal modeling software SIMM, or by using age-specific averaged parameter values for the subjects in the present study (MEAN).

because of generic optimal fiber and slack lengths, which caused significant errors and large inter-subject standard deviations. Because the generic models used the same force-length, force-extension, and force-velocity relations for all subjects, the model's ability to account for inter-individual differences was eliminated.

Limitations

As with any model, simplifications and assumptions were made. We attempted to strike a balance between model complexity and ease of interpretation. The optimized TA properties represent those of multiple muscles in the anterior compartment lumped together. The GA and SO models include the effects of other plantarflexor muscles (e.g., tibialis posterior), and contributions from the medial and lateral heads of the GA were combined. We assumed planar rotation about the ankle joint, and that the foot was rigid with no movement within the individual tarsal bones. This was reasonable with the use of the rigid dynamometer foot plate, although small changes in the ankle axis of rotation could still occur.⁴⁵

We assumed that muscle model excitation levels instantly rose to a maximum and remained there,

based on our observations of measured EMG in the isometric and isovelocity conditions. Previous work has shown no age-related differences in the ability to maximally excite muscles in either isometric or isovelocity movements.⁴¹ In addition, the model did not account for possible antagonistic co-contraction,¹¹ and therefore the modeled forces could be underestimated.

The force-length relation was a simplified parabolic version of the sarcomere force-length relation,²⁷ and we did not account for possible changes in the optimal contractile component length as a function of activation.³⁶ We did not include pennation angle effects in the simulations, although this factor was considered in the PCSA calculations. These effects would be minor due to the shape of the cosine function (e.g., even at 25° pennation, ~90% force is transmitted in the direction of the tendon). The muscle models did not include history dependence, such as force depression following muscle fiber shortening¹⁸ or enhancement following lengthening.¹⁹ This omission would cause only small time-dependent estimation errors in the predictions of muscle force during the simulations.

Due to ethical considerations, we are unable to compare model muscle force and mechanical properties with actual *in vivo* measurements. It has been shown that musculoskeletal models are particularly sensitive to errors in estimating moment arms³⁵ and PCSA.⁹ A sensitivity analysis for the effects of Hill-type muscle model parameters on musculoskeletal model results⁵⁴ demonstrated that the most sensitive parameters were those defining the maximal isometric muscle force (P_0), the eccentric plateau (ϵ), the force-length relation (L_0 and W), and the series-elastic element elasticity (L_S and K). For the comparison of subject-specific and generic prediction errors we changed all muscle properties together; the effect of changing a single property to its generic value was not tested.

CONCLUSIONS

This study demonstrated significant age-related changes in the mechanical properties of the dorsiflexors and individual plantarflexor muscles. Muscular properties were computed using a combination of joint measurements, muscle imaging, musculoskeletal modeling, and numerical optimization. It was shown that for maximum predictive power, musculoskeletal models should be tailored to individual subjects.

APPENDIX

Each muscle-tendon unit was represented by a two-component Hill-type³² model. This phenomenological lumped-parameter model incorporated a contractile

element (CE) in series with an elastic element (SEE). The behavior of the CE was defined by excitation–activation, force–length, and force–velocity relations. The behavior of the SEE was defined by a force–extension relation. Both force–length and force–velocity relations were linearly scaled with activation.

Excitation–Activation Relationship

An exponential characterized the relationship between the excitation input to the muscle model and the activation of the CE.⁷ Upon receiving an excitatory input μ , the time-course for rising CE activation λ was

$$\lambda_i = \lambda_{i-1} + \left[\mu_i \left(1 - e^{(-\Delta t/\tau)} \right) (\mu_i - \lambda_{i-1}) \right] \quad (\text{A1})$$

where i denotes the sample number, Δt is the time-step, and τ is a time constant specifying the rate of activation.

Force–Length Relationship

The isometric force producing potential of the CE (FP) depended on the maximal isometric force capability of the CE (P_0), the activation (λ), and normalized CE length (L_{CE}/L_0). The latter specifies the position on the force length relation, which is defined as an inverted parabola with width coefficient W , such that

$$FP = P_0 \lambda \left[100 W \left(\frac{L_{CE}}{L_0} - 1 \right)^2 + 1 \right] \quad (\text{A2})$$

Force–Velocity Relationship

The force–velocity relation was defined by a rectangular hyperbola based on Hill,³³ which has been shown in many experimental preparations.^{4,13,14} The shape of this relation is determined by the constants a and b , which can be expressed as normalized values a/P_0 and b/L_0 .³³ If the instantaneous force generated by the CE (P) is less than FP the CE must be shortening, such that

$$v_{CE} = - \left[\frac{(FP + a)b}{(P + a)} - b \right] \quad (\text{A3})$$

where v_{CE} is the CE velocity. If P is greater than FP , the CE must be lengthening. Therefore, based on FitzHugh²²

$$v_{CE} = \frac{b[(FP \cdot \varepsilon) - FP](FP - P)}{(FP + a)[P - (FP \cdot \varepsilon)]} \quad (\text{A4})$$

where ε is the saturation force for an eccentric contraction (eccentric plateau).

Force–Extension Relationship

The amount of SEE extension for a given force relative to the SEE slack length L_S , i.e., the stiffness,

was defined by a second-order polynomial. The length of the SEE (L_{SEE}) was given by

$$L_{SEE} = \frac{L_S}{2P_0\alpha} \left(2P_0\alpha - P_0\beta + \sqrt{P_0^2\beta^2 + 4P_0\alpha P} \right) \quad (\text{A5})$$

where α and β are coefficients defining the shape of the polynomial.

Muscle Model Force Change

The rate of change of muscle force with respect to time is given by

$$\frac{dP}{dt} = \frac{\sqrt{P_0^2\beta^2 + 4P_0\alpha P}}{L_S} \cdot v_{SEE} \quad (\text{A6})$$

where v_{SEE} is the velocity of the SEE, given by

$$v_{SEE} = v_{MT} - v_{CE} \quad (\text{A7})$$

where v_{MT} is the velocity of the musculotendon complex. During model simulation, this force change was integrated to give the muscle force at the next time step.

ACKNOWLEDGMENTS

This research was supported by NIH grant R03AG026281. We would like to thank Jeff Gagnon for assistance with muscle modeling.

REFERENCES

- ¹Agur, A. M., V. Ng Thow Hing, K. A. Ball, E. Fiume, and N. H. McKee. Documentation and three dimensional modelling of human soleus muscle architecture. *Clin. Anat.* 16:285–293, 2003.
- ²Arnold, E. M., S. R. Ward, R. L. Lieber, and S. L. Delp. A model of the lower limb for analysis of human movement. *Ann. Biomed. Eng.* 38:269–279, 2010.
- ³Bahler, A. S. Series elastic component of mammalian skeletal muscle. *Am. J. Physiol.* 213:1560–1564, 1967.
- ⁴Bahler, A. S. Modeling of mammalian skeletal muscle. *IEEE Trans. Biomed. Eng.* 15:249–257, 1968.
- ⁵Baumgartner, R. N., D. L. Waters, D. Gallagher, J. E. Morley, and P. J. Garry. Predictors of skeletal muscle mass in elderly men and women. *Mech. Ageing Dev.* 107:123–136, 1999.
- ⁶Blanpied, P., and G. L. Smidt. The difference in stiffness of the active plantarflexors between young and elderly human females. *J. Gerontol.* 48:M58–M63, 1993.
- ⁷Bobbert, M. F., and G. J. van Ingen Schenau. Isokinetic plantar flexion: experimental results and model calculations. *J. Biomech.* 23:105–119, 1990.
- ⁸Bojsen-Moller, J., P. Hansen, P. Aagaard, U. Svantesson, M. Kjaer, and S. P. Magnusson. Differential displacement of the human soleus and medial gastrocnemius aponeuro-

- ses during isometric plantar flexor contractions in vivo. *J. Appl. Physiol.* 97:1908–1914, 2004.
- ⁹Brand, R. A., D. R. Pedersen, and J. A. Friederich. The sensitivity of muscle force predictions to changes in physiologic cross-sectional area. *J. Biomech.* 19:589–596, 1986.
- ¹⁰Buchanan, T. S., D. G. Lloyd, K. Manal, and T. F. Besier. Estimation of muscle forces and joint moments using a forward-inverse dynamics model. *Med. Sci. Sports Exerc.* 37:1911–1916, 2005.
- ¹¹Caldwell, G. E., and A. E. Chapman. The general distribution problem: a physiological solution which includes antagonism. *Hum. Mov. Sci.* 10:355–392, 1991.
- ¹²Chino, K., T. Oda, T. Kurihara, T. Nagayoshi, K. Yoshikawa, H. Kanehisa, T. Fukunaga, S. Fukashiro, and Y. Kawakami. In vivo fascicle behavior of synergistic muscles in concentric and eccentric plantar flexions in humans. *J. Electromyogr. Kinesiol.* 18:79–88, 2008.
- ¹³Close, R. Dynamic properties of fast and slow skeletal muscles of the rat after nerve cross-union. *J. Physiol.* 204:331–346, 1969.
- ¹⁴Close, R. I. Dynamic properties of mammalian skeletal muscles. *Physiol. Rev.* 52:129–197, 1972.
- ¹⁵Cook, C., and M. McDonagh. Force responses to controlled stretches of electrically stimulated human muscle-tendon complex. *Exp. Physiol.* 80:477–490, 1995.
- ¹⁶Delp, S. L., J. P. Loan, M. G. Hoy, F. E. Zajac, E. L. Topp, and J. M. Rosen. An interactive graphics-based model of the lower extremity to study orthopaedic surgical procedures. *IEEE Trans. Biomed. Eng.* 37:757–767, 1990.
- ¹⁷Diffie, G. M., V. J. Caiozzo, R. E. Herrick, and K. M. Baldwin. Contractile and biochemical properties of rat soleus and plantaris after hindlimb suspension. *Am. J. Physiol. Cell Physiol.* 260:C528–C534, 1991.
- ¹⁸Edman, K. A., C. Caputo, and F. Lou. Depression of tetanic force induced by loaded shortening of frog muscle fibres. *J. Physiol.* 466:535–552, 1993.
- ¹⁹Edman, K. A., G. Elzinga, and M. I. Noble. Enhancement of mechanical performance by stretch during tetanic contractions of vertebrate skeletal muscle fibres. *J. Physiol.* 281:139–155, 1978.
- ²⁰Enoka, R. M. Eccentric contractions require unique activation strategies by the nervous system. *J. Appl. Physiol.* 81:2339–2346, 1996.
- ²¹Epstein, M., and W. Herzog. *Theoretical Models of Skeletal Muscle*. New York: Wiley, 1998.
- ²²FitzHugh, R. A model of optimal voluntary muscular control. *J. Math. Biol.* 4:203–236, 1977.
- ²³Frontera, W. R., D. Suh, L. S. Krivickas, V. A. Hughes, R. Goldstein, and R. Roubenoff. Skeletal muscle fiber quality in older men and women. *Am. J. Physiol. Cell Physiol.* 279:C611–C618, 2000.
- ²⁴Fukashiro, S., M. Rob, Y. Ichinose, Y. Kawakami, and T. Fukunaga. Ultrasonography gives directly but noninvasively elastic characteristic of human tendon in vivo. *Eur. J. Appl. Physiol. Occup. Physiol.* 71:555–557, 1995.
- ²⁵Fukunaga, T., K. Kubo, Y. Kawakami, S. Fukashiro, H. Kanehisa, and C. N. Maganaris. In vivo behaviour of human muscle tendon during walking. *Proc. R. Soc. B* 268:229, 2001.
- ²⁶Garner, B. A., and M. G. Pandy. Estimation of musculo-tendon properties in the human upper limb. *Ann. Biomed. Eng.* 31:207–220, 2003.
- ²⁷Gordon, A. M., A. F. Huxley, and F. J. Julian. The variation in isometric tension with sarcomere length in vertebrate muscle fibres. *J. Physiol.* 184:170–192, 1966.
- ²⁸Harman, S. M., E. J. Metter, J. D. Tobin, J. Pearson, and M. R. Blackman. Longitudinal effects of aging on serum total and free testosterone levels in healthy men. *J. Clin. Endocrinol. Metab.* 86:724–731, 2001.
- ²⁹Hasson, C. J., J. A. Kent-Braun, and G. E. Caldwell. Contractile and non-contractile tissue volume and distribution in ankle muscles of young and older adults. *J. Biomech.* 44:2299–2306, 2011.
- ³⁰Hasson, C. J., R. H. Miller, and G. E. Caldwell. Contractile and elastic ankle joint muscular properties in young and older adults. *PLoS One* 6:e15953, 2011.
- ³¹Henriksson-Larsén, K. B., J. Lexell, and M. Sjöström. Distribution of different fibre types in human skeletal muscles. I. Method for the preparation and analysis of cross-sections of whole tibialis anterior. *Histochem. J.* 15:167–178, 1983.
- ³²Hill, A. V. The heat of shortening and the dynamic constants of muscle. *Proc. R. Soc. B* 126B:136–195, 1938.
- ³³Hill, A. V. *First and Last Experiments in Muscle Mechanics*. London: Cambridge Press, 1970.
- ³⁴Hof, A. L. Muscle mechanics and neuromuscular control. *J. Biomech.* 36:1031–1038, 2003.
- ³⁵Hoy, M. G., F. E. Zajac, and M. E. Gordon. A musculo-skeletal model of the human lower extremity: the effect of muscle, tendon, and moment arm on the moment-angle relationship of musculotendon actuators at the hip, knee, and ankle. *J. Biomech.* 23:157–169, 1990.
- ³⁶Huijing, P. A. Important experimental factors for skeletal muscle modelling: non-linear changes of muscle length force characteristics as a function of degree of activity. *Eur. J. Morphol.* 34:47–54, 1996.
- ³⁷Jakobsson, F., K. Borg, L. Edström, and L. Grimby. Use of motor units in relation to muscle fiber type and size in man. *Muscle Nerve* 11:1211–1218, 1988.
- ³⁸Johnson, M. A., J. Polgar, D. Weightman, and D. Appleton. Data on the distribution of fibre types in thirty-six human muscles: an autopsy study. *J. Neurol. Sci.* 18:111–129, 1973.
- ³⁹Kannus, P., M. Paavola, and L. Józsa. Aging and degeneration of tendons. In: *Tendon Injuries: Basic Science and Clinical Medicine*, edited by N. Maffulli, P. Renström, and W. B. Leadbetter. London: Springer, 2005, pp. 25–31.
- ⁴⁰Kent-Braun, J. A., and A. V. Ng. Specific strength and voluntary muscle activation in young and elderly women and men. *J. Appl. Physiol.* 87:22–29, 1999.
- ⁴¹Klass, M., S. Baudry, and J. Duchateau. Aging does not affect voluntary activation of the ankle dorsiflexors during isometric, concentric, and eccentric contractions. *J. Appl. Physiol.* 99:31–38, 2005.
- ⁴²Lanza, I. R., T. F. Towse, G. E. Caldwell, D. M. Wigmore, and J. A. Kent-Braun. Effects of age on human muscle torque, velocity, and power in two muscle groups. *J. Appl. Physiol.* 95:2361–2369, 2003.
- ⁴³Larsson, L., X. Li, and W. R. Frontera. Effects of aging on shortening velocity and myosin isoform composition in single human skeletal muscle cells. *Am. J. Physiol.* 272:C638–C649, 1997.
- ⁴⁴Loram, I. D., C. N. Maganaris, and M. Lakie. Paradoxical muscle movement in human standing. *J. Physiol.* 556:683–689, 2004.

- ⁴⁵Lundberg, A., O. Svensson, G. Nemeth, and G. Selvik. The axis of rotation of the ankle joint. *J. Bone Joint Surg. Br.* 71:94–99, 1989.
- ⁴⁶Maganaris, C. N., V. Baltzopoulos, and A. J. Sargeant. In vivo measurements of the triceps surae complex architecture in man: implications for muscle function. *J. Physiol.* 512(Pt 2):603–614, 1998.
- ⁴⁷Maganaris, C. N., V. Baltzopoulos, and A. J. Sargeant. Changes in the tibialis anterior tendon moment arm from rest to maximum isometric dorsiflexion: in vivo observations in man. *Clin. Biomech.* 14:661–666, 1999.
- ⁴⁸Morgan, D. New insights into the behavior of muscle during active lengthening. *Biophys. J.* 57:209–221, 1990.
- ⁴⁹Narici, M. V., C. N. Maganaris, N. D. Reeves, and P. Capodaglio. Effect of aging on human muscle architecture. *J. Appl. Physiol.* 95:2229–2234, 2003.
- ⁵⁰Ochala, J., W. R. Frontera, D. J. Dorer, J. Van Hoecke, and L. S. Krivickas. Single skeletal muscle fiber elastic and contractile characteristics in young and older men. *J. Gerontol. A Biol. Sci. Med. Sci.* 62:375–381, 2007.
- ⁵¹Ochala, J., D. Lambertz, M. Pousson, F. Goubel, and J. V. Hoecke. Changes in mechanical properties of human plantar flexor muscles in ageing. *Exp. Gerontol.* 39:349–358, 2004.
- ⁵²Out, L., T. G. Vrijkotte, A. J. van Soest, and M. F. Bobbert. Influence of the parameters of a human triceps surae muscle model on the isometric torque–angle relationship. *J. Biomech. Eng.* 118:17–25, 1996.
- ⁵³Rugg, S. G., R. J. Gregor, B. R. Mandelbaum, and L. Chiu. In vivo moment arm calculations at the ankle using magnetic resonance imaging (MRI). *J. Biomech.* 23:495–501, 1990.
- ⁵⁴Scovil, C. Y., and J. L. Ronsky. Sensitivity of a Hill-based muscle model to perturbations in model parameters. *J. Biomech.* 39:2055–2063, 2006.
- ⁵⁵Shao, Q., D. N. Bassett, K. Manal, and T. S. Buchanan. An EMG-driven model to estimate muscle forces and joint moments in stroke patients. *Comput. Biol. Med.* 39:1083–1088, 2009.
- ⁵⁶Simoneau, E., A. Martin, and J. Van Hoecke. Effects of joint angle and age on ankle dorsi- and plantar-flexor strength. *J. Electromyogr. Kinesiol.* 17:307–316, 2007.
- ⁵⁷Spoor, C. W., J. L. van Leeuwen, W. J. van der Meulen, and A. Huson. Active force–length relationship of human lower-leg muscles estimated from morphological data: a comparison of geometric muscle models. *Eur. J. Morphol.* 29:137–160, 1991.
- ⁵⁸Storn, R., and K. Price. Differential evolution—a simple and efficient adaptive scheme for global optimization over continuous spaces. Technical Report TR-95-012, International Computer Science Institute, 1995.
- ⁵⁹Thelen, D. G. Adjustment of muscle mechanics model parameters to simulate dynamic contractions in older adults. *J. Biomech. Eng.* 125:70–77, 2003.
- ⁶⁰Toursel, T., L. Stevens, and Y. Mounier. Evolution of contractile and elastic properties of rat soleus muscle fibres under unloading conditions. *Exp. Physiol.* 84:93–107, 1999.
- ⁶¹Wickiewicz, T. L., R. R. Roy, P. L. Powell, and V. R. Edgerton. Muscle architecture of the human lower limb. *Clin. Orthop. Relat. Res.* 179:275–283, 1983.
- ⁶²Wilkie, D. R. The relation between force and velocity in human muscle. *J. Physiol.* 110:249–280, 1950.
- ⁶³Winters, J. M. Hill-based muscle models: a systems engineering perspective. In: *Multiple Muscle Systems: Biomechanics and Movement Organization*, edited by J. M. Winters, and S. L.-Y. Woo. New York: Springer, 1990, pp. 69–93.
- ⁶⁴Woittiez, R. D., P. A. Huijting, and R. H. Rozendal. Influence of muscle architecture on the length-force diagram. A model and its verification. *Pflugers Arch.* 397:73–74, 1983.
- ⁶⁵Zajac, F. E. Muscle and tendon: properties, models, scaling, and application to biomechanics and motor control. *Crit. Rev. Biomed. Eng.* 17:359–411, 1989.